THE JOURNAL OF PHYSICAL CHEMISTRY A

 VOLUME 109, NUMBER 44, NOVEMBER 10, 2005

ARTICLES

Spin Dynamics of the Radical Pair in a Low Magnetic Field Studied by the Transient Absorption Detected Magnetic Field Effect on the Reaction Yield and Switched External Magnetic Field

Toshiaki Suzuki, Tomoaki Miura, Kiminori Maeda,*,† and Tatsuo Arai*

Department of Chemistry, University of Tsukuba, 1-1-1 Tennodai, Tsukuba, Ibaraki, 305-8571, Japan

Received: July 19, 2005; In Final Form: September 11, 2005

xxThe spin dynamics of the radical pair generated from the photocleavage reaction of (2,4,6-trimethylbenzoyl)-diphenylphosphine oxide (TMDPO) in micellar solutions was studied by the time-resolved magnetic field effect (MFE) on the transient absorption (TA) and by a novel technique, absorption detected switched external magnetic field (AD-SEMF). Thanks to the large hyperfine coupling constant ($A = 38$ mT), a characteristic negative MFE on the radical yield was observed at a magnetic field lower than 60 mT whereas a positive effect due to the conventional hyperfine (HFM) and relaxation mechanisms (RM) was observed at higher magnetic field. The negative effect can be assigned to the mechanism "so-called" *low field effect* (LFE) mechanism and has been analyzed thoroughly using a model calculation incorporating a fast spin dephasing process. The time scale of the spin mixing process of LFE studied by AD-SEMF is shorter than the lifetime of the recombination kinetics of the radical pair. These results indicate that the LFE originates from the coherent spin motion. This can be interfered from the fast spin dephasing caused by electron spin interaction fluctuations.

1. Introduction

Magnetic field effects (MFE) on radical pairs have received great attention.[1] The MFE can be explained by a spin mixing process and spin selective chemical reactions and its mechanisms are categorized by the types of spin mixing processes. Generally, the MFE of the radical pair in a micelle has been explained by the mixture of two different mechanisms, the hyperfine mechanism (HFM)[1] by isotropic hyperfine interaction and the relaxation mechanism (RM)[2] due to the longitudinal electron spin relaxation by fluctuation of the anisotropic dipolar interactions of electron−nuclear and electron−electron spins. Because the time scales of HFM (about 10 ns) and RM (100 ns to 1 μs) are different, the separate observation of those spin mixing processes by time-resolved spectroscopic methods can be considered. Such observations are useful in the discussion of the more precise nature of the spin dynamics. However, very few experimental studies incorporating this concept have been performed.

The time-domain analysis of the spin mixing process of the radical pair in a micelle is difficult because the response time of the MFE on radical species is determined by the time scale of the recombination kinetics. For long-lived radical pairs, time-resolved MARY (magnetic field effect on reaction yield) experiments (application of a static magnetic field) give some approximate information on time domains. In the transient absorption (TA) experiment the MFE is a time integration of the difference of the transient concentration of the singlet radical

* To whom correspondence should be addressed. Physical & Theoretical Chemistry Laboratory, Oxford University, South Parks Road, Oxford, OX13QZ, United Kingdom. E-mail: Kiminori.maeda@chem.ox.ac.uk

† Present address: Physical & Theoretical Chemistry Laboratory, Oxford University, South Parks Road, Oxford, OX13QZ, United Kingdom.

10.1021/jp053989q CCC: $30.25
Published on Web 10/13/2005

pair with and without the magnetic field. The MFE increases with the time scale of radical pair recombination. Therefore, the time response of transient-absorption detected TR-MARY to the spin mixing is limited by the recombination kinetics. This is in contrast to the fluorescence detected TR-MARY, in which the response of the emission to the singlet radical pair formation is very quick. To solve this problem, we have used a switched external magnetic field (SEMF) technique. This technique has been developed by Bagryanskaya et al. with CIDNP observation.[3−6] In the present paper, we demonstrate a new technique, transient-absorption detected SEMF (AD-SEMF).[7]

The *low field effect* (LFE) is a unique MFE proposed to occur at very weak magnetic fields, weaker than the hyperfine coupling constant.[8−10] The LFE can be categorized as being due to the HFM, and results from the interference of coherent spin motion by hyperfine interactions and the external magnetic field. The LFE mechanism is of interest because it is one of the most probable mechanisms of the magnetic navigation of animals.[11−13] In the previous studies, the LFE has been distinctly observed brightly in the electron-transfer reactions,[14] photocleavage reaction,[15] and the ionization by pulse radiolysis[16] and vacuum ultraviolet irradiation[17] in homogeneous solutions. In micelles, the observation of LFE for the radical pairs is dependent on the observed system and was observed in the special conditions.[18−20] In addition, it is sometime difficult to distinguish the LFE mechanism from the contribution of S−T mixing mechanism caused by the exchange interaction.[21] These facts imply that the coherent spin motion would be interfered by the spin dephasing process by fluctuating spin−spin interactions.[8,9] Therefore, for the discussion of the relationship between the LFE and the spin dephasing, it is necessary to use the system that clearly shows the LFE.

The photochemical reaction of (2,4,6-trimethylbenzoyl)-diphenylphosphine oxide (TMDPO) fulfills the above-mentioned conditions and was used in the present study. This reaction produces the radical pair of diphenylphosphonyl radical and trimethylbenzoyl radical. The MFE study on the transient absorption (TA) in high magnetic field[22] and the time-resolved ESR measurements in various magnetic fields[23,24] have been performed to study the confined radical pair in the SDS micelle. Diphenylphosphonyl radical has a large hyperfine interaction ($A[^{31}P] = 38.5$ mT) and trimethylbenzoyl radical has a negligibly small hyperfine interaction.[23−25] These conditions create the most promising conditions to observe the LFE in the micellar solution and the data can be simply analyzed and modeled with theoretical calculations because the radical pair is reduced to a simple two-electron and one-nuclear spin system. In the present paper, we investigate the effect of the magnetic fields on the radical pair dynamics in the micellar solutions. We wish to describe how the spin dynamics of the radical pair can be resolved from the TR-MARY spectra and the time shift experiments of AD-SEMF.

2. Method and Materials

2-1. Materials. TMDPO (Aldrich Chem. Co.) was used after recrystallization from mixed solution hexane and ethyl acetate. Distilled water (KISHIDA Reagent Chemicals, liquid chromatography grade) was used as received. Sodium dodecyl salfate (SDS, KISHIDA Reagent Chemicals, protein analysis grade) and dodecyltrimethylammonium chloride (DTAC, Tokyo chemical reagent, normal grade) were used as received.

All transient absorption experiments were carried out in SDS or DTAC micellar solution. Concentration of TMDPO was adjusted to 5.0×10^{-4} M, and concentrations of surfactants were adjusted to 5.0×10^{-2} M. The experiments were performed under argon saturated conditions by purging. To eliminate the effect of secondary reactions, the sample solution was excited for a single laser pulse, and after excitation the solution was discarded.

2-2. Time-Resolved MARY Spectroscopy. The TA spectra were observed by a setup made in house.[26,27] A flow system was used to transfer the sample solutions into a quartz optical cell (4 mm square) where the reactions were initiated by a laser pulse. A Nd:YAG Laser (Spectra Physics GCR-3 $\lambda = 266$ nm) was used as an excitation source. The probe light generated from a 500 W Xe lamp (Ushio UXL-500SX) passed through the sample cell in the perpendicular direction of the laser pulse and the light was guided to the front of the slit of a monochromator (JASCO CT-25). The TA signal was detected by a photomultiplier (Hamamatsu R-928) attached to the monochromator. The signal from the photomultiplier is recorded by a digital oscilloscope (LeCroy LT-344) and analyzed by a personal computer (Epson Direct).

2-3. TA-Detected SEMF (AD-SEMF) Experiment. All the apparatus for TA-detected SEMF (AD-SEMF) measurement was identical to TR-MARY spectroscopy setup except for the modification of the sample cell and the redesign of the optical path of the reference light.[7] A flow system was used to transfer the sample into the quartz optical cell where the sample solution was irradiated by a laser pulse. Probe light from a Xe lamp was guided to the sample cell by an optical quartz fiber, the edge of which is fixed in the solution to illuminate the sample perpendicular to the excitation light. The transmitted light through the sample solution was guided to a monochromator by another optical quartz fiber of the same diameter.

Two identical magnetic field pulse generators have been made by ARTEK Corp. on the basis of the paper by Lin et al.[28] One pulse generator provides up to 100 A of current to a triple turned coil that is situated on the side of the sample tube. Two coils (SEMF coil) situated on both sides of the sample cell are each connected to the pulser and generate the pulsed magnetic field under the static magnetic field generated by a electric magnet (TOKIN). The rise time and the maximum amplitude of the pulsed magnetic field are 20 ns and 32 mT, respectively.[7]

Two types of the switching experiments, addition and subtraction of external magnetic field, were performed by changing installation of the SEMF coil. Addition experiments were performed by switching on the two pulse generators that provides additional magnetic field (ΔB) at a fixed delay after the laser flash under the static magnetic field (B_0). Therefore, the external magnetic field was switched from B_0 to $B_0 + \Delta B$. The subtraction experiment was performed by setting the two SEMF coils was situated such that cancellation of the static magnetic field was possible. This setting provides a switching from $B_0 + \Delta B$ to B_0.

3. Theory

Theoretical calculations have been performed for fitting of the experimental data of TR-MARY spectra and the time profiles of the MFE. The spin dynamics of the radical pair is represented by a density ket $|\sigma\rangle$, and its time evolution has been calculated by the following modified Liouville equation.

$$\frac{d|\sigma\rangle}{dt} = -iH^x|\sigma\rangle + \hat{R}|\sigma\rangle + \hat{W}|\sigma\rangle + \hat{K}|\sigma\rangle \qquad (1)$$

The first term in the right-hand side of eq 1 is the superoperator

that represents the commutator of the *spin Hamiltonian* $\hat{H}$ and the density matrix $\sigma(t)$ in the Hilbert space as shown

$$H^{\times}|\sigma\rangle \Rightarrow [H,\sigma(t)] = \hat{H}\,\sigma(t) - \sigma(t)\hat{H} \tag{2}$$

where the spin Hamiltonian $\hat{H}$ is written by

$$\hat{H} = \hat{H}_{\mathrm{Z}} + \hat{H}_{\mathrm{HFI}} + \hat{H}_{J} \tag{3}$$

$$\hat{H}_{\mathrm{Z}} = \frac{g_a \mu_{\mathrm{B}} B}{\hbar}\hat{\mathrm{S}}_{\mathrm{Z}}{}^{a} + \frac{g_a \mu_{\mathrm{B}} B}{\hbar}\hat{\mathrm{S}}_{\mathrm{Z}}{}^{b} \tag{3a}$$

$$\hat{H}_{\mathrm{HFI}} = A_a \cdot \hat{\mathrm{S}}_a \cdot \hat{\mathrm{I}}_a \tag{3b}$$

$$\hat{H}_{J} = -J\left(\frac{1}{2} + 2\hat{\mathrm{S}}_a \cdot \hat{\mathrm{S}}_b\right) \tag{3c}$$

where $\hat{H}_{\mathrm{Z}}$ and $\hat{H}_{\mathrm{HFI}}$ represent Zeeman interactions of electron spin a and b with external magnetic field B and Hyperfine interaction between electron spin a and nuclear spin in the diphenylphosphonyl radical. $\hat{H}_J$ represents the exchange interaction by the effective value J.

In our system, the radical pair consists of a diphenylphosphonyl radical and a trimethylbenzoyl radical. In our calculations we take into account only the one nuclear spin that is coupled with the electron spin, this is because the hyperfine coupling constants for another nuclei are negligibly small. This feature is one of the advantages of this system because a one nuclear spin system enables us to calculate the electron and nuclear spin dynamics without approximations. This is in contrast to multinuclear systems when the dimension of the density matrix is too large to calculate by simple quantum mechanical calculation. One of the most useful approximations for the multinuclear system is the semiclassical model proposed by Shulten et al.[29] However, the semiclassical model is not suitable for studying the LFE because this is essentially caused by quantum mechanical coherent motions of both electron and nuclear spins. In the calculations, the values used for the g factor and hyperfine coupling constant of the diphenylphosphonyl radical are (g_a = 2.0034, A = 38.5 mT) and the g factor of trimethylbenzoyl radical (g_b = 2.0006) comes from ESR data.[23−25]

$\hat{R}$ represents the spin relaxations of each radicals and is given by

$$\hat{R} = \{R_a \otimes I_b + R_b \otimes I_a\} \tag{4}$$

where $R_{a,b}$ and $I_{a,b}$ represent the electron spin relaxation matrices of radicals a and b and identity matrices for the electron spin space of radicals a and b, respectively. We assume that the spin relaxation originates from the anisotropic hyperfine interaction. The longitudinal and transverse spin relaxation rate constants can be formulated by

$$\frac{1}{T_1} = \frac{\tau_{\mathrm{c}}}{6}\frac{[A{:}A]}{1 + \omega_{\mathrm{e}}{}^{2}\tau_{\mathrm{c}}{}^{2}} \tag{5}$$

$$\frac{1}{T_2} = \frac{1}{2T_1} + \frac{\tau_{\mathrm{c}}[A{:}A]}{12} \tag{6}$$

under the high field approximation,[30] where τ_{c} and $[A{:}A]$ are rotational correlation time and anisotropy of the hyperfine coupling constants of the radical, respectively.

The HFI anisotropy $[A{:}A]$ and the correlation time of diphenylphosphonyl radical in SDS micelle have been determined by Ananchenko et al. to be 230 mT^2 and 45 ps, respectively.[31]

The high field approximation for the spin relaxation is not valid at low magnetic field because in the low field condition, the eigenstate of the spin Hamiltonian does not quantize in the Z direction of the external magnetic field. Therefore, the value of T_1 and T_2 cannot be correctly defined in low magnetic field region. Recently, Fedin et al.[32] calculated the description of the spin relaxation by an anisotropic hyperfine interaction in a low magnetic field. They calculated the eigenstates of the spin Hamiltonian at low field and formulated the spin relaxation matrix element between each eigenstate of the radical under the perturbation approximation. They also calculated the effect of the correction of the spin relaxation on MARY spectra. Their calculation shows that the LFE is always slightly overestimated if we use the matrix with the high field approximation, but not significant to change the spectral shape of MARY. This result indicates that the LFE is due to a faster spin mixing process than to the spin relaxation of the radical in micelle. We have therefore used the high field approximation in our calculation for simplicity.

In our calculation, we have not taken into account the stochastic modulation of the exchange interaction and the dipolar interaction caused by the mutual motion of the radical pair in explicit form. Instead of that, we effectively added the terms of the spin dephasing. The spin dephasing in the radical pair can be considered as two types of the dephasing phenomena, STD (singlet−triplet dephasing) and TTD (triplet−triplet dephasing).[33−36] STD is caused by the fluctuation of the exchange interaction due to the re-encounter process of the radical pair. The superoperator for STD is given by[33−34]

$$\hat{W}_{\mathrm{STD}} = -w_{\mathrm{STD}}\sum_{j=0,\pm1}(|ST_j\rangle\langle ST_j| + |T_jS\rangle\langle T_jS|) \tag{7}$$

The TTD is caused by the fluctuation of the electron spin dipole−dipole interaction (DDI). Because the interaction is anisotropic, the fluctuation is responsible for the re-encounter process and the whole rotation of the radical pairs. The contribution of TTD is expressed by[35]

$$\hat{W}_{\mathrm{TTD}} = -w_{\mathrm{TTD}}\sum_{j\neq i}(|T_iT_j\rangle\langle T_iT_j| + |T_jT_i\rangle\langle T_jT_i|) \tag{8}$$

For the simplicity, we have used the same value w for our simulation

$$w_{\mathrm{STD}} = w_{\mathrm{TTD}} = w \tag{9}$$

This assumption does not have any physical meaning because in the calculation w_{STD} and w_{TTD} cause very similar effects on the MARY spectra. Therefore, we cannot distinguish those two parameters from the simulation of our experimental results. The mechanism of dephasing is discussed later.

The chemical reaction of the radical pair is described in the Hilbert space by

$$\hat{K}|\sigma\rangle \Rightarrow -(k_{\mathrm{esc}} + k_{\mathrm{scav}})\sigma(t) - \frac{1}{2}k_{\mathrm{rec}}(P_{\mathrm{s}}\sigma(t) + \sigma(t)P_{\mathrm{s}}) \tag{10}$$

where k_{rec} and k_{esc} are the rate constants of the recombination and the escape from micelle, respectively, and P_{s} is the projection operator to the singlet electron spin state. k_{scav} is a rate constant of the scavenging of the radical pair that contains

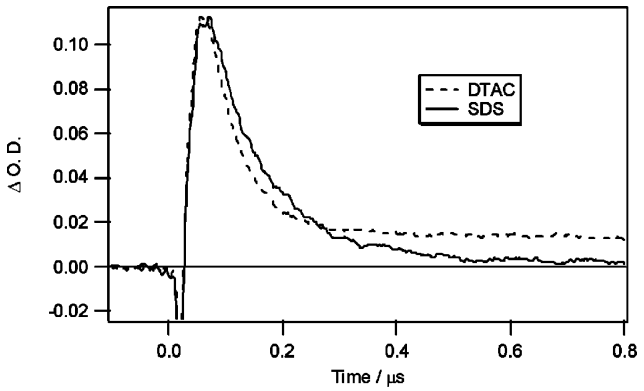

Figure 1. Decay profiles of transient absorption in the system of TMDPO observed at 340 nm (a) in SDS micelle and (b) in DTAC micelle.

the reaction with surfactant molecules and/or the recombination reaction by SOC induced intersystem crossing.[37−40]

We have used the initial condition

$$|\sigma(t=0)\rangle = \frac{1}{3}(|T_+T_+\rangle + |T_0T_0\rangle + |T_-T_-\rangle) = |\frac{3}{4} + S_a \cdot S_b\rangle \quad (11)$$

and the time evolution of the density ket is calculated by the numerical solution of eq 1. The observation value is a sum of the concentration of radical pair and that of escaped free radical and is expressed by

$$A(t) \propto tr\sigma(t) + k_{esc}\int_0^t tr\sigma(\tau)d\tau \quad (12)$$

We have calculated this value as the function of the external magnetic field, B_0 and obtained the time-resolved MARY spectra. The simulation has been performed by MATLAB (Mathworks Co. Ltd) and the determination of the parameters has been done by the automatic fitting program supplied by this language.

4. Results

Time profiles of the transient absorption of diphenylphosphonyl radical observed at 340 nm are shown in Figure 1. Because the dissociation of TMDPO takes place within 0.2 ns,[41] the TA signal of the triplet excited state and the rising feature of the radical species can be neglected because they occur within the pulse duration of the laser pulse and the dead time due to the fluorescence and/or scattered laser light. We compared the time profiles of the diphenylphosphonyl radical in SDS micelle and DTAC micellar solutions. Whereas the two types of the micelle in our study have similar diameters (R = 16.5−17.5 Å),[42] the time profiles are different in the different types of micelles. In SDS, the absorption monotonically decayed with a lifetime of 120 ns. In DTAC solution, the radical species decays can be best fitted to a double-exponential function with lifetimes of 60 ns and 2.5 μs. The short-lived decay components of nanosecond time scales are assigned to the recombination process of the geminate radical pair confined in micelles. The slow decay component observed in DTAC solution can be assigned to the decay of the free radicals that has escaped from the micelle or has stayed in micelle after escape of the partner radical. It is interesting that the escaping process in SDS micelle is negligibly small, but the escaped radical is observable in DTAC micelle. This is due to the different boundary character of the micelles formed by the different hydrophilic headgroups.

The recombination reaction rate constant from the singlet radical pair has been estimated to be 4 times that of the observed

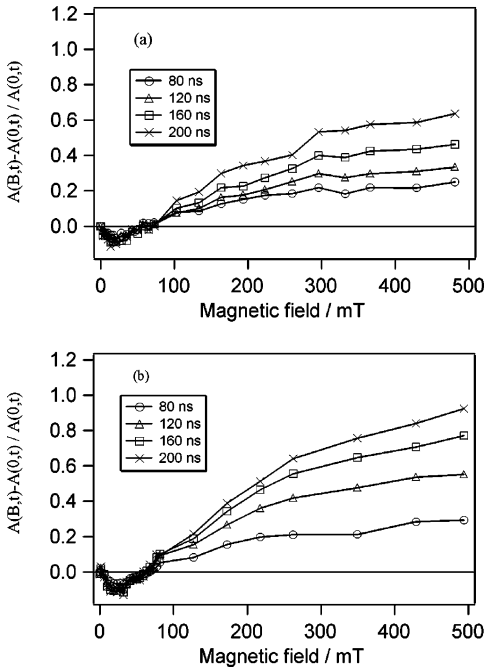

Figure 2. Time-resolved MARY spectra of TMDPO in SDS (a) and in DTAC micelle (b).

decay rate constant of radical pair in zero magnetic field; this estimate comes from the fact that only the singlet state (which is only one-fourth of the radical generated) recombines to produce the products, assuming the spin mixing process is faster than the recombination kinetics. The recombination rate constants from the singlet radical pair in both micelles are tentatively estimated to be $k_{rec} = 3.2 \times 10^7$ s^{-1} in the SDS micelle and $k_{rec} = 6.7 \times 10^7$ s^{-1} in the DTAC micelle, respectively.

The time-resolved MARY spectra can be plotted by the calculation of the magnetic field effect $E(B,t)$ as follows.

$$E(B,t) = \frac{A(B,t) - A(0,t)}{A(0,t)} \quad (13)$$

where $A(B,t)$ and $A(0,t)$ are the transient absorption signals in the presence and the absence of an external magnetic field, respectively.

The time-resolved MARY spectra of the photoreaction of TMDPO in SDS micellar solution are shown in Figure 2a. In the low field region up to 60 mT, a negative MFE appears in the spectra. Generally, a negative dip in MARY spectra had often been explained by the contribution of the level crossing mechanism (LC mechanism) due to T−S mixing.[1] However, in the present system, this is not reasonable because the observed peak position of the negative effect is similar to the hyperfine coupling constant of phosphonylradical. Therefore, the negative effect observed around 30 mT can be rationalized by the LFE.

Owing to the large hyperfine coupling constant of phosphonyl radical, we could observe a clear and strong LFE on the radical pair in micelles. From the viewpoint of a general discussion of the MFE on biological systems including such phenomena as animal navigations, the LFE observed at about 30 mT is not really the *low field* because animal sensing occurs in the earth magnetic field at only ∼0.04 mT. However, from a physical and theoretical viewpoint, the present MFE is useful as the model of LFE for studying the spin dynamics.

At high magnetic field (over 60 mT) the observed MFE (HF-MFE) is positive, as shown in Figure 2. The direction of the MFE observed at high magnetic field can be rationalized as

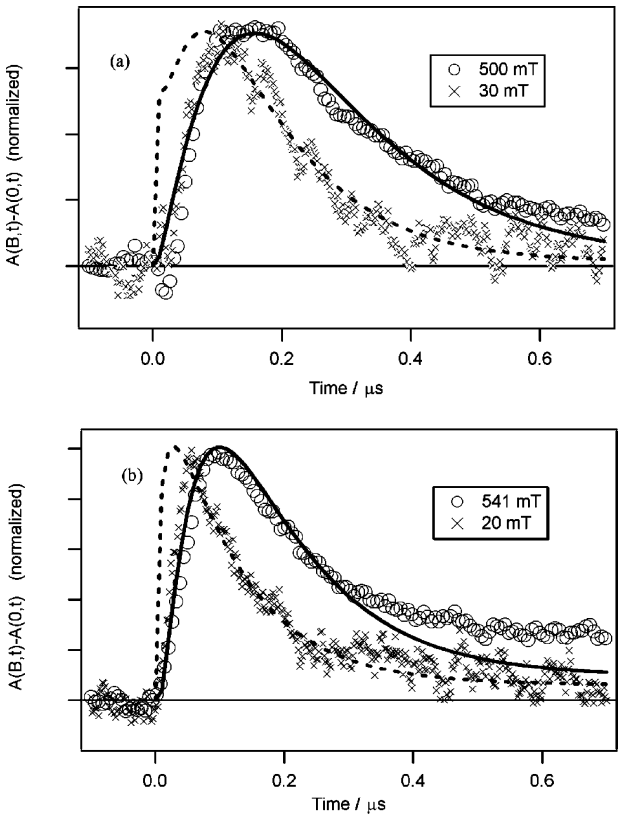

Figure 3. Normalized time profile of MFE in photocleavage of TMDPO at low magnetic field (○) and high magnetic field (×) in SDS micelle (a) and in DTAC micelle (b). The solid and broken lines are the results of the theoretical calculations.

the HFM and the RM. It is distinctive that the MFE at high field grows up after the laser flash, in contrast to the LFE, which appears immediately and does not have any evolution at longer times, as shown in Figure 2. In the DTAC micelle, a similar time-resolved MARY spectrum is observed except that the absolute value and the time evolution feature of the HF-MFE is different, as shown in Figure 2b. The absolute intensity of the HF-MFE is larger than that observed in SDS.

The time profile of the MFE has been obtained by a subtraction of the time profile observed in zero magnetic field, $A(t,0)$ from that in arbitrary magnetic field given by

$$P(t,B) = A(t,B) - A(t,0) \tag{14}$$

The normalized time profiles observed at low magnetic field (LFE: $B = 30$ mT) and high magnetic field (HF-MFE: $B = 500$ mT) in SDS micelles are shown in Figure 3. The LFE in SDS increases up to 110 ns after laser pulse and then decays whereas HF-MFE decays in a relatively longer time scale, as shown in Figure 3a. The difference of the time profiles between LFE and HF-MFE is caused by the difference of the time scale of the spin mixing processes. In the DTAC micelle, the difference of the MFE time profiles are more striking as shown in Figure 2b. This difference is due to the different recombination kinetics. In the DTAC micelle, the recombination rate constant is twice as large as that in SDS micelle. Therefore, in the DTAC micelle, the difference of the spin mixing time scale between LFE and HF-MFE appears more sharply on the difference of the time profiles of MFE.

For an improvement of signal-to-noise ratio of TR-MARY spectra, we have accumulated the data in the low field region (0−90 mT), and the results are shown in Figure 4. The spectra have been simulated by the theoretical calculation described in section 3. We have reproduced the time evolution of the spectral shape (solid line in Figure 4) by using a fast dephasing rate constant, $w = 5 \times 10^8$ s^{-1}. The details of the simulation result are discussed in the next section.

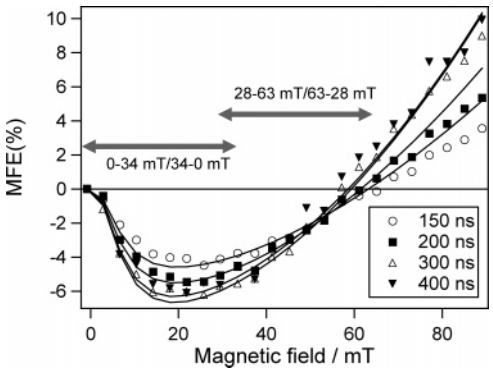

Figure 4. Time-resolved MARY spectra observed in SDS micelle by focusing on the low field region. The solid line is the result of the model simulation using appropriate parameters: $J = -2$ mT, $w = 5 \times 10^8$ s^{-1}, $k_{rec} = 6 \times 10^7$ s^{-1}, and $k_{scav} = 1 \times 10^6$ s^{-1}.

The results of the AD-SEMF shift experiments are shown in Figure 5. Figure 5a shows the schematic diagram of the AD-SEMF experiment. After laser irradiation, the external magnetic field was switched from B_0 to $B_0 + \Delta B$ and vice versa. The effect of the switching of the magnetic field on the change of the transient absorption, $\Delta A(\text{on}) - \Delta A(\text{off})$, in the time region of 100−400 ns was averaged after switching (shadow in the figure), and plotted as a function of the delay time of the switching, t_D.

Figure 5b is the result that has been obtained by the switching from 0 to 34 mT (0−34 mT) and the opposite switching (34−0 mT). In this switching range of the magnetic field, the negative LFE increases with increasing magnetic field, as shown in Figure 4. The time profile of the switching experiment should reflect the time scale of the spin mixing process that induces the LFE. We have analyzed the time profiles by fitting the decays to single-exponential functions. The time constants for 34−0 and 0−34 mT are 53 and 78 ns, respectively. In the second region, in which the positive HF-MFE increases with increasing magnetic field, the time profiles have decays longer than those for the LFE and their time constants are 114 ns for 28−63 mT and 120 ns for 63−28 mT, as shown in Figure 5c.

5. Discussion

5-1. Time Profiles of MFE Observed at Low Magnetic Field and High Magnetic Field. In this section, we discuss the time profiles of the LFE and the HF-MFE. Our calculations of the quantum mechanical spin dynamics have indicated that the HFM on the singlet character of the radical pair spin state appears on a time scale of subnanoseconds, which is about 10 times shorter than that in the system of usual carbon centered organic radicals (∼10 ns).[43] The LFE is based on the coherent electron spin motion by hyperfine interaction and a small external magnetic field. Therefore, LFE should be sensitive to the dephasing process by the fluctuation of the spin interactions. The theoretical discussion by Brocklehurst has suggested that the transverse spin relaxation (T_2) quenches the LFE.[8,9] Recently, Monte Carlo calculations by O'Dea et al. show that the motion of the radical pair is one of the origin of the quenching of LFE.[44] Concerning the suggestion of the theoretical works, we can expect that the spin mixing for the LFE will have a time scale shorter than that of HF-MFE.

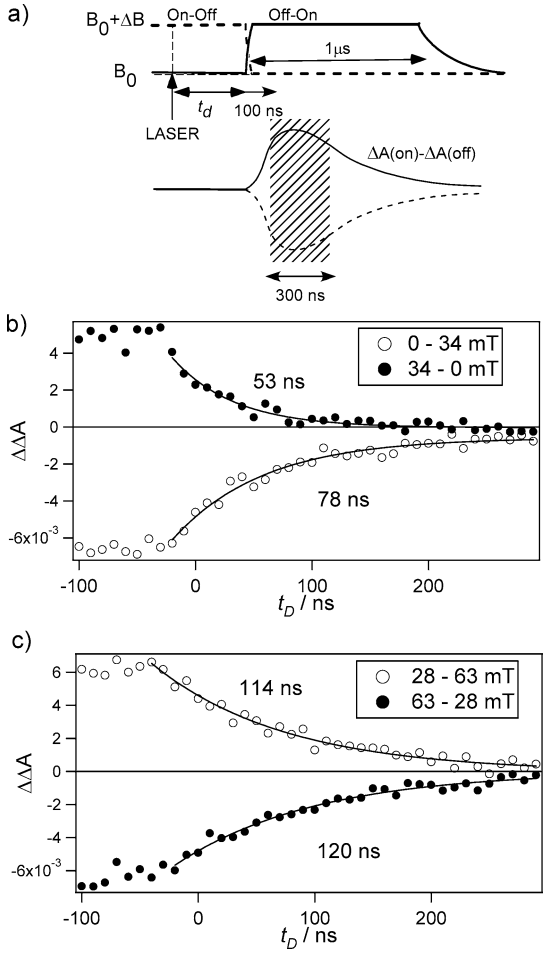

Figure 5. (a) Schematic representation of the AD-SEMF shift experiment. t_D is the delay time of the magnetic field switching after laser irradiation. The effect of the pulsed magnetic field on TA signal in the time region from 100 to 400 ns after switching has been averaged and has plotted versus t_D. (b) Time profiles obtained by the AD-SEMF shift experiment. Switching range is 0 to 34 mT for open circles and 34 to 0 mT for filled circles. The solid lines are fitting curves by single-exponential function and the obtained time constants are printed on the side. (c) The switching range is 28 to 63 mT for open circles and 63 to 28 mT for filled circles. The solid lines are fitting curves by single-exponential function and the obtained time constants are printed on the side.

The difference of the time scale between LFE and HF-MFE is reflected in the time profiles of MFE, as shown in Figure 3. However, the observed time profiles have been broadened in time through the relatively slow recombination kinetics. When we compare the results in SDS and DTAC, the difference of the time profiles between LFE and HF-MFE is more striking in DTAC. As discussed above, the response of the MFE on the TA signal is determined by the rate constant of the recombination process from the singlet radical pair. Therefore, in the system of DTAC, the MFE time profile has a quicker response to the spin mixing process because the k_{rec} is twice as fast as that in the system of SDS.

The model calculations reproduce the experimentally observed time profiles as shown in Figure 3. The optimized recombination rate constants are $k_{rec} = 3.6 \times 10^7\ s^{-1}$ for the SDS micelle and $k_{rec} = 7.0 \times 10^7\ s^{-1}$ for the DTAC micelle. These values are similar to those obtained by the decay kinetics of TA observed at zero magnetic field. The discrepancies of the theoretical curve in Figure 3 within 80 ns after laser flash are due to the intervention of emission signals from the experimental conditions (Figure 1).

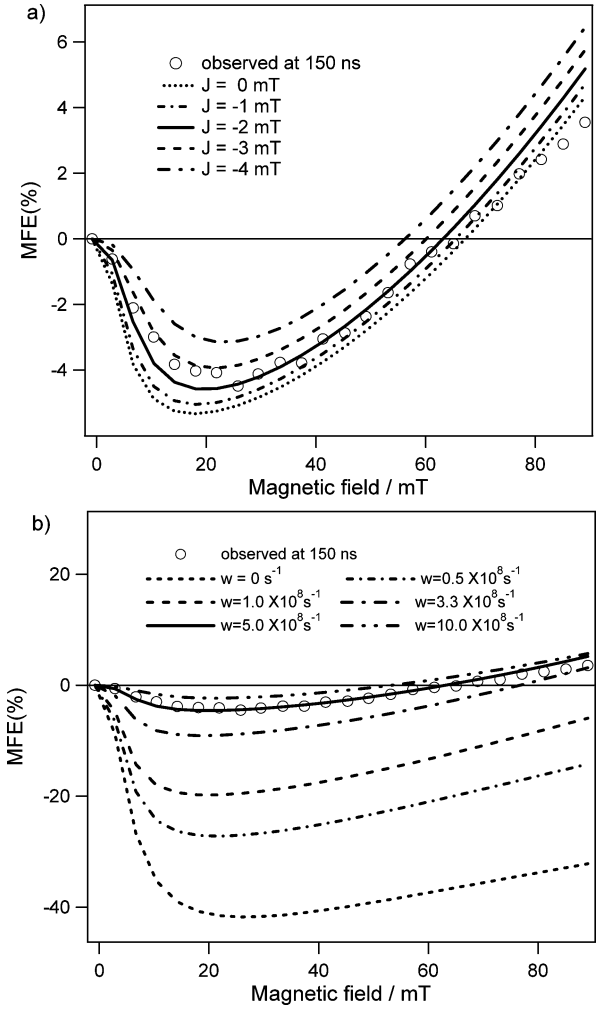

Figure 6. Effect of the essential parameters, J and w, on the MARY spectra: (a) J dependence on the calculation of MARY; (b) w dependence on the calculation of MARY. The other parameters are same with that in Figure 4.

5-2. MARY Spectra. We have studied the time-resolved MARY spectra and compared the results with theoretical calculations. The MARY spectrum calculated by the model described above is shown in the solid lines in Figure 4. The MARY curve in the low magnetic field region, in which the MARY mainly originates from LFE, is very sensitive to both the exchange interaction J and the dephasing parameter w. The MARY curve calculated with various values of J is shown in Figure 6a. An increase of the absolute value of J results in a decrease in the LFE component. This result is striking because it is opposite to what is expected if the level crossing mechanism (LC mechanism) were the origin of the negative MFE. In general for radical pair systems it is probable that the LC mechanism produces a similar MARY curve. However, this occurs when the splitting of the singlet and triplet radical pairs ($-2J$) is larger than the hyperfine interactions and the peak position of the negative MFE is $2|J|$. In the present case, the hyperfine coupling constant is much larger than the exchange interaction, which has been observed by CIDEP experiments.[23,24] In addition, the peak position of the observed negative MFE is comparable to the hyperfine coupling constant of the diphenyl phosphonyl radical. In such a case, the LFE mechanism should be the origin of the negative MARY curve rather than the LC mechanism.

The effect of the dephasing rate w on the calculated MARY spectra is shown in Figure 6b. The results clearly show that the dephasing mechanism is responsible for the spectral shape of

MARY. In the previous experimental and theoretical studies the dephasing rate constant, *w*, of the radical pairs in a micelle has been regarded as the order of the re-encounter frequency, that is, the order of 10^7 to 10^8 s^{-1}.[23,34−36]

We have optimized the two parameters (*J* and *w*) by using the automatic fitting program. The fitting results are shown in the solid lines in Figure 4. The optimized parameters of *J* and *w* values are −2 mT and 5×10^8 s^{-1}, respectively. We have also used the kinetic parameters $k_{rec} = 6 \times 10^7$ s^{-1} and $k_{scav} = 1 \times 10^6$ s^{-1}, which do not change the spectral shape of MARY curve in the low field region effectively but model the time evolution of the spectra. The observed *w* value is similar to the value observed by the decay of the transient nutation of the radical pair detected by ADMR technique in the same system by Yashiro et al.[45]

The dephasing phenomena in the radical pair have been reported by several groups. In the micellar system, Tarasov et al. have shown the effect of the fluctuation of the exchange interaction on SNP[21,46] and CIDEP[23,47] spectra based on the theory of Shushin[33,34] and Alexandrov et al.[36] In addition, Maeda et al.[48] have observed a unusually large broadening of the ADMR spectra in the polymethylene-linked system of xanthone and xanthene under the spin locking condition. This broadening was explained by Gorelik et al. as the effect of TTD due to the anisotropy of electron−electron and/or electron−nuclear dipole−dipole interaction by the precise analysis of the high power and the pulsed ADMR experiments.[35] In a system of the electron-transfer reaction in homogeneous solutions, PCDMR (photoconductivity detected magnetic resonance) spectral shape in a high microwave field also reflects the contribution of TTD or T_2 relaxation.[49]

The simulation by the model calculation indicates that the fast dephasing decreases the LFE. This fact is one of the reasons the LFE has been hardly observed in the micellarized radical pair with a small hyperfine coupling constant.[17] In contrast, the LFE has clearly been observed in homogeneous solution.[15,50] In the homogeneous solutions the radical pair lifetime is so short that the LFE is not affected by the spin dephasing.

Our calculations based on the single site model in the present analysis are a useful practical method for fitting the experimentally observed MARY data. However, this model has limitations. First we have used a Redfield matrix on the basis of a perturbation theory under the high field approximation. It is still questionable whether the perturbation theory is applicable when the energy splitting of the eigenstate is comparable to the fluctuating perturbation by the anisotropic hyperfine interactions. Fedin et al. has developed a relaxation theory by anisotropic hyperfine interaction in low fields by calculating the eigenstates of the spin Hamiltonian.[28] This theory is, however, still in the category of a perturbation approximation. We conclude, however, that the dephasing mechanism is more efficient mechanism for describing the spectral shape of MARY spectra in the low field region.

The other limitation of our simulation is that we have used an effective parameter for the dephasing of the radical pair spin dynamics. The observed dephasing parameter should reflect the fluctuation of the spin interactions due to the molecular dynamics. The analysis by stochastic Liouville equation[46,47] and/or Monte Carlo[44] calculations that take into account the fluctuation of the exchange and the anisotropic interactions would be useful for the discussion of the relationship of the LFE and the molecular dynamics. Such calculation requires a lot of CPU time and memory. Moreover, there are many unknown modeling and its parameters of the molecular motion in the micelle.

5-3. AD-SEMF Experiment. The time-resolved measurements of the MFE have a limited time resolution for the spin mixing process because of the broadening by the recombination kinetics and the dead time due to the interference by emission or scattered light. This problem can be overcome if the time scale of the spin mixing process is measured by means of the shift experiment of SEMF. However, if the spin mixing dynamics of the quasi-steady state is observed, the time profile of AD-SEMF should be identical to the time profile of the radical pair. Comparing the AD-SEMF time profiles in radical pair systems with small hyperfine coupling constants (in which the LFE was hardly observed) revealed that the time profiles were identical to those observed by TA experiment in the same magnetic field before the switching of the magnetic field in the SEMF experiment.[51] In the pulsed RYDMR experiments in high magnetic field (∼330 mT), the spin mixing is the same and the results of the microwave shift experiments show clearly the spin relaxation and the escape kinetics of the radical pairs.[52,53] These facts indicate that the HF-MFE of the radical pair in the micelle is generally due to the second-order electron spin polarization of the radical pair in a quasi steady state of populations, which is determined by the relation between the spin relaxation and the recombination kinetics of the radical pair. The polarization in the quasi-steady state is proportional to the concentration of the radical pair, which can be observed using the TA method.

In the present system of TMDPO, the similar time constants with the TA lifetimes have been observed in the switching experiment of 28−63 and 63−28 mT. In this region the positive slope of the MARY spectra is due to the HF-MFE. Therefore, the SEMF reflects the population decay of the radical pair in the quasi steady state. In contrast, the time profiles of the switching experiment of 0−34 mT and 34−0 mT show time constants (∼60 ns) shorter than the lifetime of the radical pair (∼120 ns). This fact is a novel feature in that previous similar techniques such as pulsed RYDMR and CIDNP−SEMF did not observe in a long lived radical pair. It is because it is the transient and coherent spin dynamics of the radical pair from the quasi steady state of the radical pair spin states that is being observed.

Previous theoretical studies[8−10] suggest that the LFE originates from the coherent spin dynamics in the radical pair and is quenched by the spin dephasing phenomena. The observed short time constant of the AD-SEMF in low field region (0−34 mT and 34−0 mT) supports these theoretical suggestions. The pulse width (∼10 ns) of the laser pulse and the rise time of the SEMF (∼20 ns) are comparable to those of the observed SEMF decays, and therefore a more quantitative discussion about the time scale of the spin mixing is not possible. However, the theoretical simulation that take these factors into account may be helpful for discussions of the effect of spin dephasing on the LFE.

5-4. Origin of the Dephasing. The spin dephasing phenomena is a crucial component in determining the spectral shape of MARY with LFE mechanism. That diminishes the LFE contribution effectively. It is interesting to determine the origin of the fast spin dephasing in a micelle. However, it is difficult because it was not possible to obtain the parameters of w_{STD} and w_{TTD} from MARY spectra, independently. There are three possible origins: *J* modulation (STD), electron−electron dipolar spin interaction (TTD by DDI), and electron−nuclear (anisotropy of HFI). The modulation of the anisotropy of HFI contributes to both STD and TTD. As discussed above, the contribution of the anisotropy of HFI should be small if the

assumption of the Redfield theory were valid. The contribution of the DDI on the electron spin dephasing is a subject for discussion. About the high field MFE, Steiner et al. calculated the effect of the dipole−dipole interaction on the T_1 relaxation of the radical pair and showed that the contribution of DDI is small on the radical pair dynamics in a micelle.[54] However, for the LFE, the Monte Carlo calculation by O'Dea et al.[44] showed that the LFE is eliminated by DDI. More experimental results from various systems are required before definite conclusions can be made.

Acknowledgment. We express our grateful acknowledgment to Prof. M. Wakasa for preliminary experiment of this work, and to Prof. P. J. Hore, Dr. C. R. Timmel, and Dr. K. Henbest for stimulating discussion of this work. This work was supported by a Grant-in-Aid for Development of Scientific Research (No. 13740320) from the Japan Society for the Promotion of Science and a Grant-in-Aid for Scientific Research on Priority Areas (417) from the Ministry of Education, Culture, Sports, Science and Technology (MEXT) of the Japanese Government. K.M. is indebted to Yazaki Memorial Foundation for Science & Technology, the Kao Foundation for Arts and Sciences, Casio Science Promotion Foundation, and Saneyoshi Foundation. T.A. is grateful to a financial support by the Asahi Glass Foundation.

References and Notes

(1) Steiner, U. E.; Ulrich, T. *Chem. Rev.* **1989**, *89*, 51.
(2) Hayashi, H.; Nagakura, S. *Bull. Chem. Soc. Jpn.* **1984**, *57*, 322.
(3) Parnachev, A. P.; Purtov, P. A.; Bagryanskaya, E. G.; Sagdeev, R. Z. *J. Chem. Phys.* **1997**, *107*, 9942.
(4) Bagryanskaya, E. G.; Gorelik, V. R.; Sagdeev, R. Z. *Chem. Phys. Lett.* **1997**, *264*, 655.
(5) Fedin, M. V.; Purtov, P. A.; Bagryanskaya, E. G. *J. Chem. Phys.* **1999**, *111*, 5491.
(6) Fedin, M. V.; Bagryanskaya, E. G.; Purtov, P. A.; Makarov, T. N.; Paul, H. *J. Chem. Phys.* **2002**, *117*, 6148.
(7) Miura, T.; Maeda, K.; Arai, T. To be published.
(8) Brocklehurst, B. *J. Chem. Soc., Faraday Trans.* **1976**, *72*, 1869.
(9) Brocklehurst, B.; McLauchlan, K. A. *Int. J. Radiat. Biol.* **1996**, *69*, 3.
(10) Timmel, C. R.; Till, U.; Brocklehurst, B.; Mclauchlan, K. A.; Hore, P. J. *Mol. Phys.* **1998**, *95*, 71.
(11) Ritz, T.; Adem, Schulten, K. *Biophys. J.* **2000**, *78*, 707.
(12) Ritz, T.; Thalau, P.; Philips, J. B.; Wiltschko, W. *Nature* **2004**, *429*, 177.
(13) Cintolesi, F.; Ritz, T.; Kay, C. W. M.; Timmel, C. R.; Hore, P. J. *Chem. Phys.* **2003**, *294*, 385.
(14) Hamilton, C. A.; Hewitt, J. P.; McLauchlan, K. A.; Steiner, U. E. *Mol. Phys.* **1988**, *65*, 423.
(15) Vink, C. B.; Woodward, J. R. *J. Am. Chem. Soc.* **2005**, *51*, 16730.
(16) Stass, D. V.; Tadjikov, B. M.; Molin, Y. N. *Chem. Phys. Lett.* **1995**, *235*, 511.
(17) Saik, V. O.; Lipsky, S. *Chem. Phys. Lett.* **1997**, *264*, 649.
(18) Eveson, R. W.; Timmel, C. R.; Brocklehurst, B.; Hore, P. J.; McLauchlan, K. A. *Int. J. Radiat. Biol.* **2000**, *76*, 1509.
(19) Tarasov, V. F.; Shkrob, I. A.; Step, E. N.; Buchachenko, A. I. *Chem. Phys.* **1989**, *135*, 391.
(20) Shkrob, I. A.; Tarasov, V. F.; Buchachenko, A. I. *Chem. Phys.* **1991**, *153*, 443.
(21) Tarasov, V. F.; Ghatlia, N. D.; Avdievich, N. I.; Turro, N. J. *Z. Phys. Chem.* **1993**, *182*, 227.
(22) Hayashi, H.; Sakaguchi, Y.; Kamachi, M.; Schnabel, W. *J. Phys. Chem.* **1987**, *91*, 3936.
(23) Tarasov, V. F.; Yashiro, H.; Maeda, K.; Azumi, T.; Shkrob, I. A. *Chem. Phys.* **1998**, *226*, 253.
(24) Bagryanskaya, E.; Fedin, M.; Forbes, M. D. E. *J. Phys. Chem. A* **2005**, *109*, 5064.
(25) Adrian, F. J.; Akiyama, K.; Ingold, K. U.; Wan, J. K. S. *Chem. Phys. Lett.* **1989**, *155*, 333.
(26) Murakami, M.; Maeda, K.; Arai, T. *Chem. Phys. Lett.* **2002**, *362*, 123.
(27) Murakami, M.; Maeda, K.; Arai, T. *J. Phys. Chem. A* **2005**, *109*, 5793.
(28) Sloop, D. J.; Lin, T.; Ackerman, J. J. H. *J. Magn. Reson.* **1999**, *139*, 60.
(29) Schulten, K.; Wolynes, P. G.; *J. Chem. Phys.* **1978**, *68*, 3292.
(30) Carrington, A.; McLachlan, A. D. *Introduction of Magnetic Resonance with Applications to Chemistry and Chemical Physics*; Harper & Row: New York, 1967.
(31) Ananchenko, G. S.; Bagryanskaya, E. G.; Tarasov, V. F.; Sagdeev, R. Z.; Paul, H. *Chem. Phys. Lett.* **1996**, *255*, 267.
(32) [32)] Fedin, M. V.; Purtov, P. A.; Bagryanskaya, E. G. *Chem. Phys. Lett.* **2001**, *339*, 395.
(33) Shushin, A. I. *Chem. Phys. Lett.* **1991**, *181*, 274.
(34) Shushin, A. I. *Chem. Phys.* **1990**, *144*, 201.
(35) Gorelik, V. R.; Maeda, K.; Yashiro, H.; Murai, H. *J. Phys. Chem. A* **2001**, *105*, 8011.
(36) Alexandrov, I. V.; Karamjan, L. G. *Mol. Phys.* **1972**, *24*, 1313.
(37) de Kanter, F. J. J.; Kaptein, R. *J. Am. Chem. Soc.* **1982**, *104*, 4759.
(38) Zimmt, M. B.; Doubleday, C., Jr.; Gould, I. R.; Turro, N. J. *J. Am. Chem. Soc.* **1985**, *107*, 6724.
(39) Wang, J.; Doubleday, C., Jr.; Turro, N. J. *J. Am. Chem. Soc.* **1989**, *111*, 3962.
(40) Doubleday Jr, C.; Turro, N. J.; Wang, J. *Acc. Chem. Res.* **1989**, *22*, 199.
(41) Jockusch, S.; Koptyug, I. V.; McGarry, P. F.; Sluggett, G. W.; Turro, N. J.; Watkins, D. M. *J. Am. Chem. Soc.* **1997**, *119*, 11495.
(42) Tartar, H. V. *J. Phys. Chem.* **1955**, *59*, 1195.
(43) Maeda, K.; Suzuki, T.; Arai, T. *Riken Rev.* **2002**, *44*, 85.
(44) O'Dea, A. R.; Curtis, A. F.; Green, N. J. B.; Timmel, C. R.; Hore, P. J. *J. Phys. Chem. A* **2005**, *109*, 869.
(45) Yashiro, H. Ph.D. Thesis.
(46) Tarasov, V.; Bagryanskaya, E. G.; Shkrob, I. A.; Avdievich, A. I.; Ghatlia, N. D.; Lukzen, N. N.; Turro, N. J.; Sagdeev, R. Z. *J. Am. Chem. Soc.* **1995**, *117*, 110.
(47) Tarasov, V. F.; Yashiro, H.; Maeda, K.; Azumi, T.; Shkrob, I. A. *Chem. Phys.* **1996**, *212*, 353.
(48) Maeda, K.; Araki, Y.; Kamata, Y.; Enjo, K.; Murai, H.; Azumi, T. *Chem. Phys. Lett.* **1996**, *262*, 110.
(49) Matsuyama, A.; Murai, H. *J. Phys. Chem. A* **2002**, *106*, 2227.
(50) Batchelor, S. N.; Kay, C. W.; McLauchlan, K. A.; Shkrob, I. A. *J. Phys. Chem.* **1993**, *97*, 13250.
(51) Miura, T.; Maeda, K.; Arai, T. Unpublished result.
(52) Sakaguchi, Y.; Astashkin, A. V.; Tadjikov, B. M. *Chem. Phys. Lett.* **1997**, *280*, 481.
(53) Konishi, Y.; Okazaki, M.; Toriyama, K. *J. Phys. Chem.* **1995**, *99*, 12540.
(54) Steiner, U. E.; Wu, J. Q. *Chem. Phys.* **1992**, *162*, 53.